Appl. Comput. Harmon. Anal. 26 (2009) 181–199

Contents lists available at ScienceDirect

Applied and Computational Harmonic Analysis

www.elsevier.com/locate/acha

Pointwise smoothness of space-filling functions

S. Jaffard [a], S. Nicolay [b,*]

[a] Université Paris Est, Laboratoire Analyse et Mathématiques Appliquées, 61, Avenue du Général de Gaulle, 94010 Créteil cedex, France
[b] University of Liège, Institute of Mathematics, Grande Traverse, 12, Liege, Belgium

ARTICLE INFO

Article history:
Received 21 March 2008
Accepted 8 April 2008
Available online 11 April 2008
Communicated by Yves F. Meyer

Keywords:
Hölder regularity
Space-filling functions
Multifractal formalisms

ABSTRACT

We study irregularity properties of generic Peano functions; we apply these results to the determination of the pointwise smoothness of a Peano function introduced by Lebesgue and of some related functions, showing that they are either monohölder or multifractal functions. We test on these examples several numerical variants of the multifractal formalism, and we show how a change of topology on $\mathbb{R}$ can affect the Hölder regularity of such functions.

1. Introduction

A *space-filling function* is a function $F(t) = (f(t), g(t))$, defined on $[0, 1]$, whose range fills a surface of the plane. It is called a *Peano function* if, in addition, it is continuous. These constructions were initially motivated by their paradoxical aspect. The interest in Peano functions has been periodically renewed, as unexpected connexions with several parts of mathematical analysis were discovered: They have been used as a tool that allowed to put into light nonmeasurability properties, and in connexion with the Hahn–Mazurkiewicz theorem, see [37]. In 1936, H. Steinhaus showed that space-filling functions can be obtained if their coordinates $f(t)$, $g(t)$ are stochastically independent functions, see [42]. In 1945, R. Salem and A. Zygmund discovered analytic functions in the unit disc, that have a continuous extension on the unit circle $\mathcal{C}$, and are such that the image of the unit circle is also space filling; the examples they provided were lacunary Taylor series, satisfying a strong lacunarity condition, see [38] and also [6] for later extensions. The historical developments of Peano functions, in connexion with other parts of analysis are detailed in the book of H. Sagan [37]. Another utility of Peano curves appeared at the beginning of the year 2000, in the fields of "Data Mining" and "Intelligent Data Analysis," motivated by the extensive use of large multidimensional arrays: One needs indexing of such arrays (i.e. constructing curves that go through all the points of the array) which satisfy proximity requirements: Data that are close should be indexed by close indices; this leads naturally to the use of Peano functions that satisfy some Hölder regularity conditions, see for instance [23,33]. This property of preserving the spacial relationship of 2D-patterns is also exploited in the area of digital image processing, where Peano curves are used as a scanning technique, see for instance [7,35].

Peano functions have also been popular because they supply simple geometric constructions of continuous nowhere differentiable functions. This last motivation was considerably sharpened in the last 15 years with the introduction of "multifractal analysis," where the rather imprecise motivation of nondifferentiability was replaced by the sharper requirement of determining everywhere the exact pointwise Hölder regularity. Let us recall the definitions associated with the notion of pointwise smoothness.

* Corresponding author.
E-mail address: S.Nicolay@ulg.ac.be (S. Nicolay).

1063-5203/$ – see front matter
doi:10.1016/j.acha.2008.04.002

Definition 1. Let $f:\mathbb{R}\to\mathbb{R}$ be a locally bounded function, let $x_0\in\mathbb{R}$ and $\alpha\geqslant 0$; $f\in C^\alpha(x_0)$ if there exist $R>0$, $C>0$, and a polynomial P of degree less than α such that

$$\text{if}\quad |x-x_0|\leqslant R\quad\text{then}\quad \bigl|f(x)-P(x-x_0)\bigr|\leqslant C|x-x_0|^\alpha. \tag{1}$$

The Hölder exponent of f at x_0 is $h_f(x_0)=\sup\{\alpha:\ f\in C^\alpha(x_0)\}$.

Space-filling functions can exhibit a large variety of smoothness characteristics: We will see that some of them, as shown by the initial examples supplied by Peano [34] and Hilbert [14], have everywhere the same Hölder exponent (such functions are called *monohölder functions*). But the Hölder exponent of others can present an extremely wild behavior: For example, in the case of Polya's function it is known to be everywhere discontinuous, see [20,26]. The next step in such cases is to perform a "multifractal analysis," i.e. to determine their *spectrum of singularities* which is defined as follows.

Definition 2. Let f be a locally bounded function; its isohölder sets are the sets

$$E_H=\bigl\{x_0:\ h_f(x_0)=H\bigr\}.$$

The spectrum of singularities of f is the function $d_f:\mathbb{R}^+\to\mathbb{R}^+\cup\{-\infty\}$ defined by

$$d_f(H)=\dim(E_H),$$

where dim denotes the Hausdorff dimension (using the standard convention $\dim(\emptyset)=-\infty$).

The investigation of the multifractal properties of space-filling functions goes back to [20,26], and was reactivated recently in [31]. The purpose of this paper is to derive general irregularity properties of such functions and to illustrate the variety of their smoothness behaviors by focusing on three "historical" space-filling functions, which are slight variants of each other, but present strong discrepancies from the point of view of multifractal analysis. The first one, $\mathcal{L}_1$, was introduced by H. Lebesgue in his famous monograph "Leçons sur l'intégration et la recherche de fonctions primitives," in 1904 (see [24, pp. 44–45]). We will show that it is a "monofractal function," i.e. a function which is C^∞ except on a fractal set (the triadic Cantor set $\mathcal{K}$), where its Hölder exponent takes a finite constant value. The second function, $\mathcal{L}_2$, was introduced by Schoenberg in 1938, see [39]: It coincides with Lebesgue's function on $\mathcal{K}$, but it is extended outside of $\mathcal{K}$ in such a way that it turns out to be a monohölder function. The third example is derived form $\mathcal{L}_1$ by performing a discontinuous change of time which maps the Cantor set onto the whole interval $[0,1]$. The "Lebesgue–Davenport" function $\mathcal{L}_3(t)$ thus obtained has a dense set of discontinuities, and is a simple example of "Davenport series," see (18). If the nowhere differentiability of these functions has been repeatedly considered (see [37] and references therein), nonetheless, the determination of their exact pointwise regularity, and therefore their multifractal analysis is new.

Section 2 is devoted to some general remarks on the smoothness of Peano functions. In particular, we prove there that most historical examples are monohölder functions.

Sections 3 to 5 are devoted to recall the definitions and main properties of the initial Lebesgue function and its two variants, and to determine their exact pointwise smoothness. In the case of $\mathcal{L}_3$, it will be the consequence of a new general result on the pointwise smoothness of Davenport series.

The spectrum of singularities of signals obtained through the registering of real-life data cannot be estimated in the case of multifractal signals; indeed the determination of their Hölder exponent is not numerically stable because it usually jumps at every point; on top of that, the acquisition of the spectrum would require the determination of an infinite number of Hausdorff dimensions, each of them defined by considering an uncountable number of coverings with unspecified sets. Therefore, formulas, referred to as "multifractal formalisms," have been introduced in order to derive the spectrum of singularities of a signal from numerically computable quantities. All of them are variants of a seminal derivation which was proposed by G. Parisi and U. Frisch in [32]. Though they are based on the same thermodynamic arguments, their numerical performances can vary a lot. A key step in the numerical improvements was performed by A. Arneodo and his collaborators, when they introduced formulas based on wavelet analysis, see [3]. There exists now two well established forms of multifractal formalisms, allowing to obtain the whole spectrum of singularities: The *wavelet transform maxima method* (WTMM) see [2] and references therein, and the *wavelet leaders method* (WLM) developed in [1,18,22]. The purpose of Section 7 is to compare their numerical performances on the particular case-studies supplied by the Lebesgue functions; indeed, $\mathcal{L}_1$, $\mathcal{L}_2$, and $\mathcal{L}_3$ supply a competitive benchmark for that purpose: For instance, $\mathcal{L}_1$ is linear on intervals of all possible scales (their lengths are the $(3^{-j})_{j\geqslant 1}$), which is a standard pitfall for the numerical performances of multifractal formalisms, and $\mathcal{L}_3$ has a dense set of discontinuities, a border-line situation where wavelet-based techniques are no longer backed by theoretical results, see [18].

Section 6 was initially motivated by the following problem: The notion of pointwise smoothness clearly depends on the metric used on the real line: Another distance $d(x,y)$ would induce a new definition of $C^\alpha(x_0)$, where (1) is replaced by

$$\text{if}\quad |x-x_0|\leqslant R\quad\text{then}\quad \bigl|f(x)-P(x-x_0)\bigr|\leqslant Cd(x,x_0)^\alpha. \tag{2}$$

Alternative distances introduced up to now in this context were obtained through a continuous time-change; they only induced mild modifications of the usual distance on $\mathbb{R}$, since they are topologically equivalent: Let θ be a continuous increasing one-to-one mapping $[0,1] \to [0,1]$; the distance associated with θ is

$$d_\theta(x,y) = \big|\theta(y) - \theta(x)\big|. \tag{3}$$

Such a time-change θ can strongly simplify the multifractal nature of f, see for instance [26] where it transforms the Pólya function into a monohölder function. An intriguing problem, which remains largely open, is to understand when such a simplifying time-change exists, see [40] for partial results. Functions with a dense set of discontinuities, such as $\mathcal{L}_3$ cannot be thus transformed through a continuous time-change. We will show that, using ultrametric distances on $[0,1]$, $\mathcal{L}_3$ (and more generally p-adic Davenport series) indeed becomes monohölder.

Note that the converse idea has also been used in order to generate new multifractal stochastic processes: B. Mandelbrot proposed to "complexify" a monohölder process (typically a Fractional Brownian Motion) through a multifractal time-change; these constructions were motivated by financial modeling, see [25].

2. Space-filling functions

In this section, we consider some geometric properties of space-filling functions that are commonly satisfied, and we investigate their implications in terms of pointwise smoothness. A straightforward consequence of these considerations will be the determination of the exact pointwise smoothness of several historical Peano functions. It may be useful to give precise definitions at this point: Let meas_d denote the d-dimensional Lebesgue measure. A function $f:[0,1] \to \mathbb{R}^d$ is *space-filling* if $\text{meas}_d(f([0,1])) > 0$. It is a Peano function if, additionally, it is continuous.

Uniform Hölder regularity of Peano functions $f(t) = (x(t), y(t))$ was first considered by Salem and Zygmund [38] who remarked that, if $x(t) \in C^\alpha([0,1])$ and $y(t) \in C^\beta([0,1])$, then $\alpha + \beta \leqslant 1$. As regards pointwise smoothness, M. Morayne proved that there is no space-filling everywhere differentiable function (see [30, Theorem 3, p. 131]).

The famous theorem of Netto states that there exists no bijective continuous function $f:[0,1] \to [0,1]^2$; thus continuous onto functions necessarily have multiple points. However most of these functions have a "small" set of multiple points, and therefore satisfy the following requirement.

Definition 3. Let $\text{Mult}(f)$ denote the set of points of $\mathbb{R}^d$ that have multiple antecedents by f. A function $f:[0,1] \to \mathbb{R}^d$ is almost one-to-one if

$$\text{meas}_d\big(\text{Mult}(f)\big) = 0.$$

Assume now that $f:[0,1] \to \mathbb{R}^d$ is a continuous, almost one-to-one space-filling function. A measure μ_f, supported by $[0,1]$, naturally attached to f is defined by

$$\mu_f(A) = \text{meas}_d\big(f(A)\big). \tag{4}$$

If the range of f fills a finite volume, then μ_f is a probability measure (up to a multiplicative constant).

Let $I_h(t_0) = [t_0 - h, t_0 + h]$; the pointwise Hölder exponent of a measure μ is defined by

$$h_\mu(t_0) = \liminf_{h \to 0}\left(\frac{\log(\mu(I_h(t_0)))}{\log(h)}\right).$$

Lemma 4. *Let $f:[0,1] \to \mathbb{R}^d$ be an almost one-to-one space-filling function. Let $t_0 \in [0,1]$; if $h_f(t_0) < 1$, then*

$$h_{\mu_f(t_0)} \geqslant d\, h_f(t_0). \tag{5}$$

Proof. If $f \in C^\alpha(t_0)$ for an $\alpha \in (0,1)$, then $f(I_h(t_0)) \subset B(f(t_0), Ch^\alpha)$ so that

$$\mu_f\big(I_h(t_0)\big) = \text{meas}_d\big(f\big(I_h(t_0)\big)\big) \leqslant Ch^{d\alpha};$$

one concludes by taking a log and a lim inf on both sides. □

Many usual space-filling functions present a remarkable extra feature: The range of f *covers equal volumes* (*or areas in dimension* 2) *in equal times*, i.e.

$$\text{for any interval } I, \quad \text{meas}_1(I) = \text{meas}_d\big(f(I)\big). \tag{6}$$

Functions displaying this feature include the initial Peano, and the modification proposed by Wunderlich [43], the initial Hilbert function, and the variant of Moore [29], the Sierpiński function [41] and the Pólya function in multifractal time, as presented in [26]; indeed this property is a straightforward consequence of hypothesis $(\mathcal{H})$ which is of geometric nature and, by construction, is obviously satisfied by these functions; (6) means that the measure μ is exactly the Lebesgue measure (up to a constant), and in that case, the conclusion of Lemma 4 is that the Hölder exponent of f is everywhere smaller than $1/2$. A stronger result of *uniform irregularity* holds.

Definition 5. Let $\alpha \in (0,1)$. A function $f:\mathbb{R}^d \to \mathbb{R}^m$ belongs to $I^\alpha(x_0)$ if

$$\exists C>0,\ \exists R>0,\ \forall r \leqslant R,\quad \sup_{x,y\in B(x_0,r)} \big|f(x)-f(y)\big| \geqslant Cr^\alpha; \tag{7}$$

f belongs to $I^\alpha(\mathbb{R}^d)$ if

$$\exists C>0,\ \exists R>0,\ \forall r \leqslant R,\ \forall x,\quad \sup_{y\in B(x,r)} \big|f(x)-f(y)\big| \geqslant Cr^\alpha. \tag{8}$$

Note that these types of statements are stronger than just negating Hölder regularity; indeed such negations only yield the existence of subsequences r_n for which the oscillation $\sup_{x,y\in B(x_0,r_n)}|f(x)-f(y)|$ is large, whereas (7) or (8) require the oscillation to be large at all (small enough) scales (see [9] for a comprehensive study of this notion).

Lemma 6. *Let f be a continuous function satisfying* (6); *then f belongs to $I^{1/d}([0,1])$.*

Proof. Let $0 \leqslant x < y \leqslant 1$; then

$$\sup_{s,t\in[x,y]} \big|f(x)-f(y)\big| = \operatorname{diam}\big(f\big([x,y]\big)\big) \geqslant C\big(\operatorname{meas}_d\big(f\big([x,y]\big)\big)\big)^{1/d} = C|x-y|^{1/d}. \qquad \square$$

Note that the conclusion of Lemma 6 would still hold if (6) was replaced by the less restrictive condition

$$\exists C>0\text{: for any interval } I,\quad \operatorname{meas}_1(I) \leqslant C \operatorname{meas}_d\big(f(I)\big). \tag{9}$$

Definition 7. Let $\alpha \in (0,1)$; A function $f:\mathbb{R}^d \to \mathbb{R}^m$ is strongly monohölder of exponent α ($f \in SM_\alpha$) if $f \in C^\alpha(\mathbb{R}^d) \cap I^\alpha(\mathbb{R}^d)$, i.e. if $\exists C, C'>0$, $\exists R>0$, $\forall r \leqslant R$, $\forall x$,

$$Cr^\alpha \leqslant \sup_{y\in B(x,r)} \big|f(x)-f(y)\big| \leqslant C'r^\alpha. \tag{10}$$

In general, equality needs not hold in (5) because, in the neighborhood of t_0, f may be very oscillating in one direction for instance, in which case its range will cover a very small area, though f can be very irregular. However the specific functions we mention satisfy an additional geometric requirement:

($\mathcal{H}$) There exists an integer $p \geqslant 2$ such that the image of a p^d-adic interval $I_{k,j} = \big[\frac{k}{p^{dj}}, \frac{k+1}{p^{dj}}\big]$ is a subset of volume Cp^{-dj} and of diameter $C'p^{-j}$; furthermore, for each $j \geqslant 0$ given, at scale j, all the $f(I_{k,j})$ have disjoint interiors.

Proposition 8. *Let f be a Peano function satisfying* (9) *and* ($\mathcal{H}$). *Then f belongs to $SM_{1/d}$.*

In particular, for $d=2$, this conclusion holds for the functions of Peano, Wunderlich, Hilbert, Moore, Sierpiński and the time-changed Polya function mentioned above. In particular, they are monohölder with Hölder exponents everywhere equal to $1/2$.

Proof. We only have to prove the uniform regularity estimate. Let $0 \leqslant x < y \leqslant 1$, and let j be defined by

$$p^{-dj-2} \leqslant y-x < p^{-dj}.$$

Either x and y belong to the same p^d-adic interval of generation j or to two adjacent ones. In the first case,

$$\big|f(x)-f(y)\big| \leqslant \operatorname{diam}\big(f(I_{k,j})\big) = C'p^{-j} \leqslant C'|x-y|^{1/d}.$$

In the second case, since f is continuous, the images of these two intervals share one point; but ($\mathcal{H}$) implies that

$$\big|f(x)-f(y)\big| \leqslant 2\operatorname{diam} f\big((I_{k,j})\big) = C'p^{-j}. \qquad \square$$

3. The Lebesgue function $\mathcal{L}_1$

Let $p>1$ be an integer. If $(t_i)_{i\in\mathbb{N}}$ is a sequence of integers satisfying $0 \leqslant t_i \leqslant p-1$, then

$$(0; t_1, t_2, \ldots, t_n, \ldots)_p$$

will denote the real number

$$t = \sum_{i=1}^{\infty} \frac{t_i}{p^i};$$

if the t_i are not all equal to $p-1$ for i large enough, it is the *proper expansion* of t in base p.

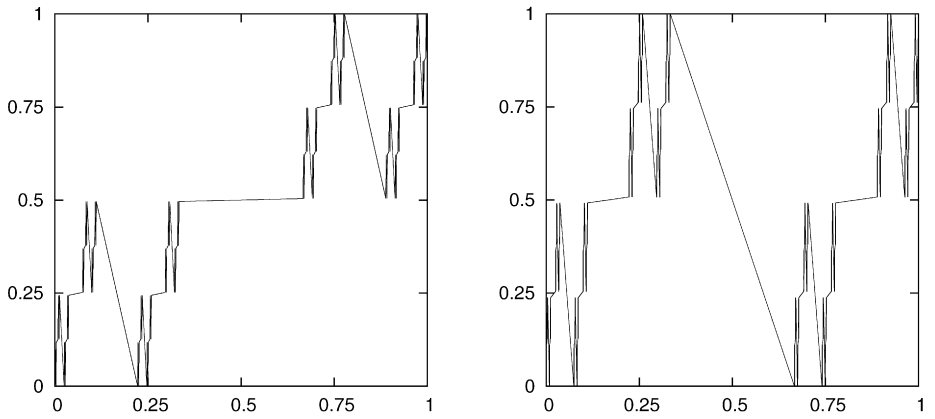

Fig. 1. The components $x_1(t)$ and $y_1(t)$ of the Lebesgue function $\mathcal{L}_1(t) = (x_1(t), y_1(t))$.

Definition 9. The triadic Cantor set $\mathcal{K}$ is the set of real numbers t that can be written

$$t = (0; 2t_1, 2t_2, \ldots, 2t_n, \ldots)_3 \quad \text{where } t_i \in \{0, 1\}, \ \forall i. \tag{11}$$

If $t \in \mathcal{K}$, then the t_i are unique (but do not necessarily constitute the proper expansion of t in base 3). Let $\mathcal{K}^*$ be the subset of $\mathcal{K}$ defined by

$$\mathcal{K}^* = \big\{t \in \mathcal{K}\colon \ (11) \text{ is the proper expansion of } t\big\}$$

($\mathcal{K}^*$ is obtained from $\mathcal{K}$ as follows: In the construction of $\mathcal{K}$ as a limsup of triadic intervals, the right-end points of each interval are eliminated).

The function $\mathcal{L}_1$ is first defined on $\mathcal{K}$ as follows. For any $t \in \mathcal{K}$ written as in (11), $\mathcal{L}_1(t) = (x_1(t), y_1(t))$ where

$$\begin{cases} x_1(t) = (0; t_1, t_3, t_5, \ldots)_2, \\ y_1(t) = (0; t_2, t_4, t_6, \ldots)_2. \end{cases} \tag{12}$$

H. Lebesgue proved that the restriction of $\mathcal{L}_1$ to $\mathcal{K}$ is an onto function onto the square $[0, 1]^2$, see [24, pp. 44–45]. We will need a slightly stronger assertion.

Lemma 10. *The restriction of $\mathcal{L}_1$ to $\mathcal{K}^*$ is an onto function onto $[0, 1]^2 - \{(1, 1)\}$.*

Proof. Let $(x, y) \in [0, 1]^2 - \{(1, 1)\}$. Then either x or y has a proper expansion starting with a 0. We use this expansion in (12), which defines a sequence t_i, hence, by (11), a point $t \in \mathcal{K}$ such that $\mathcal{L}_1(t) = (x, y)$. Since either x or y has a proper expansion, it follows that t is also written with a proper expansion, and therefore $t \in \mathcal{K}^*$. Note that this point is not necessarily unique since, if x or y is dyadic, then it can be written in the binary system in two different ways; thus points such that at least one of their coordinates are dyadic have at least two pre-images in $\mathcal{K}$ by $\mathcal{L}_1$. Note that Lebesgue's result follows since $\mathcal{L}_1(1) = (1, 1)$. □

H. Lebesgue proved that $\mathcal{L}_1$ has a continuous extension outside of $\mathcal{K}$ which is simply obtained by taking a linear extension on each interval which is a connex component of the complement of $\mathcal{K}$, thus showing that $\mathcal{L}_1$ was a new example of Peano function. The following proposition sharpens this result and yields the uniform regularity of $\mathcal{L}_1$ and its exact pointwise regularity at every point.

Proposition 11. *Let $\alpha = \frac{\log 2}{2 \log 3}$. The function $\mathcal{L}_1$ belongs to $C^\alpha([0, 1])$. If $x_0 \notin \mathcal{K}$, then $\mathcal{L}_1$ is C^∞ at x_0. If $x_0 \in \mathcal{K}$, then $\mathcal{L}_1$ belongs to $I^\alpha([0, 1])$. It is therefore a monofractal function.*

Though this proposition can be proved directly, we prefer to postpone its proof to Section 4 where it will be a consequence of the corresponding result for the Schoenberg function.

4. The Schoenberg function $\mathcal{L}_2$

Let $p(t)$ be the 2-periodic even function which satisfies on $[0, 1]$

$$\begin{cases} p(t) = 0 & \text{if } t \in [0, 1/3], \\ p(t) = 3t - 1 & \text{if } t \in [1/3, 2/3], \\ p(t) = 1 & \text{if } t \in [2/3, 1]. \end{cases}$$

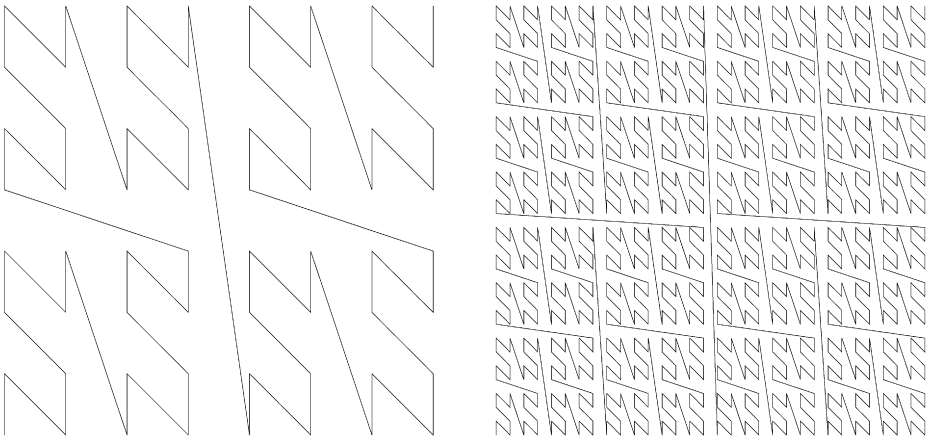

Fig. 2. The partial sums of the curve $(x_1(t), y_1(t))$ summed up to $j = 2^6$ and $j = 2^{10}$, respectively.

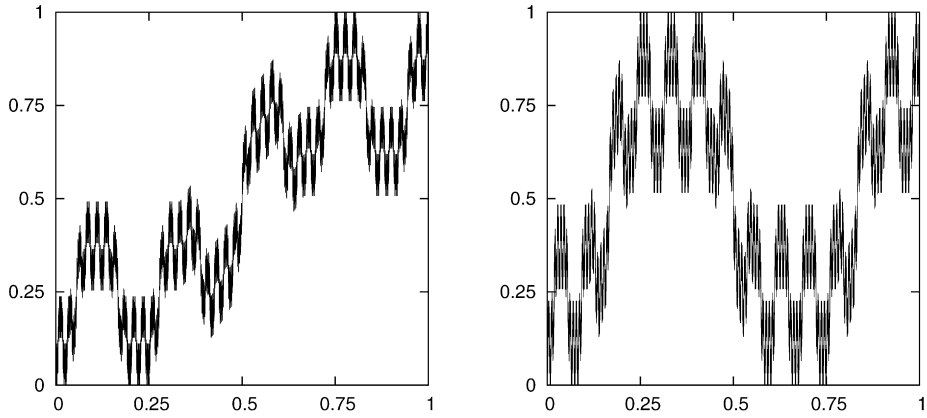

Fig. 3. The components $x_2(t)$ and $y_2(t)$ of the Schoenberg function $\mathcal{L}_2(t) = (x_2(t), y_2(t))$.

Note that p is a continuous, piecewise linear function, hence it is a Lipschitz function. The Schoenberg function $\mathcal{L}_2$ is defined by $\mathcal{L}_2(t) = (x_2(t), y_2(t))$ where

$$x_2(t) = \frac{1}{2}\sum_{n=0}^{\infty} \frac{p(3^{2n}t)}{2^n} \quad \text{and} \quad y_2(t) = \frac{1}{2}\sum_{n=0}^{\infty} \frac{p(3^{2n+1}t)}{2^n}. \tag{13}$$

The relationship between $\mathcal{L}_2$ and $\mathcal{L}_1$ was established by I. Schoenberg in 1938, see [39]:

Proposition 12. *The Schoenberg function $\mathcal{L}_2$ coincides with the Lebesgue function $\mathcal{L}_1$ on the triadic Cantor set.*

Proof. Let us first check that, if $t \in \mathcal{K}$ is written as in (11), then

$$p\big(3^n t\big) = t_{n+1}. \tag{14}$$

Indeed, let $t \in \mathcal{K}$; it follows from (11) that we can write $3^n t$ as a sum of three terms

$$3^n t = \big(2t_1 3^{n-1} + \cdots + 2t_n\big) + \frac{2t_{n+1}}{3} + \left(\frac{2t_{n+2}}{9} + \cdots\right).$$

The first term of this sum is an even integer, and the third one is positive and bounded by $1/3$; thus (14) immediately follows from the definition of $p(t)$.

It follows from (14) that

$$x_2(t) = \frac{1}{2}\sum_{n=0}^{\infty} \frac{p(3^{2n}t)}{2^n} = \frac{1}{2}\sum_{n=0}^{\infty} \frac{t_{2n+1}}{2^n} = (0; t_1, t_3, t_5, \ldots)_2;$$

Fig. 4. The curve $(x_2(t), y_2(t))$ approximated at resolution levels $j = 2^7$ and 2^9, respectively.

and similarly

$$y_2(t) = \frac{1}{2}\sum_{n=0}^{\infty} \frac{p(3^{2n+1}t)}{2^n} = \frac{1}{2}\sum_{n=0}^{\infty} \frac{t_{2n+2}}{2^n} = (0; t_2, t_4, t_6, \ldots)_2;$$

hence Proposition 12 holds. □

Lemma 10 and Proposition 12 put together imply that the Schoenberg function is also onto $[0,1]^2$. In 1981, J. Alsina [4] proved that $\mathcal{L}_2$ is nowhere differentiable (see also [15,37] for additional properties of this function). The following proposition yields its exact pointwise smoothness everywhere.

Proposition 13. *Let $\alpha = \frac{\log 2}{2\log 3}$. The Schoenberg function $\mathcal{L}_2$ belongs to SM_α.*

We will derive this proposition as a consequence of two general results: Lemma 14 yields a uniform regularity criterion and Proposition 15 yields a uniform irregularity criterion. Note that the irregularity is a consequence of results valid either for selfsimilar functions, see [16] or for Weierstrass type functions, see [8]. However, we prefer to follow an alternative approach, which will emphasize another specificity of $\mathcal{L}_2$ and yields a more straightforward proof.

Lemma 14. *Let $(f_n)_{n\in\mathbb{N}}$ be a sequence of bounded and Lipschitz functions on $\mathbb{R}$ satisfying*

$$\exists C > 0: \quad \|f_n\|_\infty + \|f_n'\|_\infty \leqslant C.$$

Let

$$f(t) = \sum_{n=0}^{\infty} \frac{f_n(b^n t)}{a_n},$$

and assume that

$$\exists C,\ a > 0 \quad \text{such that} \quad b > a > 1 \quad \text{and} \quad \forall n, \quad a_n \geqslant C a^n.$$

Then $f \in C^\beta(\mathbb{R})$ with $\beta = \frac{\log a}{\log b}$.

Proof. The assumptions on f_n imply that $|f_n(s) - f_n(t)|$ can either be bounded by C or by $C|s-t|$. Let s and t be two distinct real numbers, and let n_0 be defined by $b^{-n_0+1} < |s-t| \leqslant b^{-n_0}$; then

$$\left|f(s) - f(t)\right| \leqslant C\sum_{n=0}^{n_0} \frac{|b^n s - b^n t|}{a^n} + \sum_{n_0}^{\infty} \frac{C}{a^n} \leqslant C|s-t|\left(\frac{b}{a}\right)^{n_0} + \frac{C}{a^{n_0}} \leqslant C|s-t|^\beta.$$

The uniform regularity of $\mathcal{L}_2$ follows from Lemma 14. □

Proposition 15. *Let $f_n : \mathbb{R} \to \mathbb{R}$ be 1-periodic Lipschitz functions, of Lipschitz constants*

$$C_n = \sup_{x\neq y} \frac{|f_n(x) - f_n(y)|}{|x-y|}.$$

Let

$$f(t)=\sum_{n=0}^{\infty}\frac{f_n(b^n t)}{a_n},$$

where b is an integer satisfying $b\geqslant 2$, and the a_n satisfy

$$\exists a\in(1,b),\ \exists E_1,E_2>0\quad \text{such that}\quad E_1a^n\leqslant|a_n|\leqslant E_2a^n.$$

Let $l\in\{-b-1,\dots,b-1\}$, $D_n=f_n(\frac{l}{b})-f_n(0)$, and let $\beta=\frac{\log a}{\log b}$. Let C and D be such that, for n large enough,

$$|D_n|\geqslant D>0\quad \text{and}\quad |C_n|\leqslant C. \tag{15}$$

$$\text{If}\quad \frac{Cl}{E_1b(\frac{b}{a}-1)}<\frac{|D|}{E_2},\quad \text{then}\quad f\in I^{\beta}(\mathbb{R}).$$

Proof. First, note that the triangular inequality implies that it is sufficient to prove that the relation (8) is satisfied for couples (x,y) of the form

$$x=\frac{k}{b^{n_0}}\quad\text{and}\quad y=\frac{k+l/b}{b^{n_0}},\quad \forall(k,n_0)\in\mathbb{Z}\times\mathbb{N}.$$

In that case,

$$f(y)-f(x)=\sum_{n=0}^{n_0-1}\frac{f_n(b^n y)-f_n(b^n x)}{a_n}+\frac{D_n}{a_{n_0}}$$

(indeed, since g is 1-periodic, the increments for $n>n_0$ vanish). Since the result clearly does not depend on the first f_n, we can assume that (15) is satisfied for all n. But

$$\left|\sum_{n=0}^{n_0-1}\frac{f_n(b^n y)-f_n(b^n x)}{a_n}\right|\leqslant\sum_{n=0}^{n_0-1}\frac{C_n}{E_1}|x-y|\frac{b^n}{a^n}\leqslant\frac{C}{E_1}|x-y|\left(\frac{b}{a}\right)^{n_0}\frac{1}{\frac{b}{a}-1}\leqslant\frac{Cl}{E_1a^{n_0}b(\frac{b}{a}-1)}.$$

Since $|\frac{D_n}{a_{n_0}}|\geqslant\frac{D}{E_2\cdot a^{n_0}}$, it follows that

$$\text{if}\quad \frac{Cl}{E_1b(\frac{b}{a}-1)}<\frac{|D|}{E_2},\quad \text{then}\quad \big|f(y)-f(x)\big|\geqslant\frac{C'}{a^{n_0}};$$

hence Proposition 15 holds. □

Note that this result applies to $x_2(t)$ which is a 1-periodic function, since, in this case, $f_n(t)=p(2t)$, $C_n=C=6$, $l=3$, $D_n=D=1$, $b=9$, $a=2$ and $E_1=E_2=1$.

Let us now check how to derive Proposition 11 from Lemma 14 and Proposition 15. The regularity result is a particular case of a general regularity result for interpolating functions.

Definition 16. Let f be a continuous function on $\mathbb{R}$. Let $I_n=(a_n,b_n)$ be a sequence of two by two disjoint open intervals. The linear interpolation of f on the $(I_n)_{n\in\mathbb{N}}$ is the continuous function g defined by

- If $x\notin\bigcup I_n$, then $g(x)=f(x)$;
- g is linear on each interval $[a_n,b_n]$.

Proposition 17. *Let $\alpha\in(0,1)$ and $f\in C^{\alpha}(\mathbb{R})$. Its linear interpolation on the $(I_n)_{n\in\mathbb{N}}$ also belongs to $C^{\alpha}(\mathbb{R})$.*

Proof. Let A denote the complement of $\bigcup\overline{I_n}$. In order to estimate $g(x)-g(y)$, we separate different cases:

- If x and y both belong to A, the estimate follows from the result for f.
- If x and y both belong to the same interval I_n, then, by linear interpolation,

$$\big|g(x)-g(y)\big|=\frac{|x-y|}{|b_n-a_n|}\big|f(b_n)-f(a_n)\big|\leqslant C\frac{|x-y|}{|b_n-a_n|}|b_n-a_n|^{\alpha}\leqslant C|x-y|^{\alpha}.$$

- Let us finally assume that either x or y belongs to A, or that they belong to different intervals I_n. We can suppose that $x<y$, $x\in[a_n,b_n]$ and $y\in[a_m,b_m]$, with the convention that $a_n=b_n$ if x (for instance) does not belong to one of the I_n. Then

$$\big|g(x)-g(y)\big|\leqslant\big|g(x)-g(b_n)\big|+\big|g(b_n)-g(a_m)\big|+\big|g(a_m)-g(y)\big|;$$

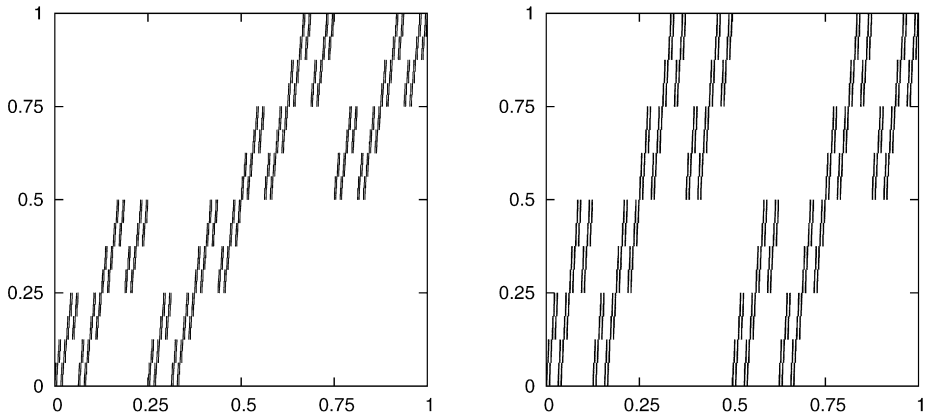

Fig. 5. The components $x_3(t)$ and $y_3(t)$ of the Lebesgue–Davenport function $\mathcal{L}_3(t) = (x_3(t), y_3(t))$.

each of these three terms has already been taken care of above. Thus

$$\big|g(x) - g(y)\big| \leqslant C\big(|x - b_n|^\alpha + |b_n - a_m|^\alpha + |a_m - y|^\alpha\big) \leqslant 3C|x - y|^\alpha. \qquad \square$$

Let us now deduce the pointwise irregularity of $\mathcal{L}_1$ from Proposition 15.

Corollary 18. *For any $x \in \mathcal{K}$, $\mathcal{L}_1 \in I^\beta(x)$.*

Proof. First, note that the proof of Proposition 15 applied to $\mathcal{L}_2$ implies that, if x and y are two endpoints of one of the triadic intervals of generation $2n$ that come up in the construction of $\mathcal{K}$, then

$$\exists C > 0: \quad \big|\mathcal{L}_2(x) - \mathcal{L}_2(y)\big| \geqslant \frac{C}{2^n}.$$

If $z \in \mathcal{K}$, then it belongs to one such interval for each n, so that, by the triangular inequality, either

$$\big|\mathcal{L}_2(x) - \mathcal{L}_2(z)\big| \geqslant \frac{C}{2^{n+1}} \quad \text{or} \quad \big|\mathcal{L}_2(z) - \mathcal{L}_2(y)\big| \geqslant \frac{C}{2^{n+1}}.$$

Since $\mathcal{L}_1$ and $\mathcal{L}_2$ coincide on $\mathcal{K}$, this implies that $\mathcal{L}_1 \in I^\beta(x)$. $\square$

5. The function $\mathcal{L}_3$ and p-adic Davenport series

The two functions we considered can be interpreted as one space-filling function defined on $\mathcal{K}$ which is extrapolated outside of $\mathcal{K}$ in two different ways. The third function we will consider can be interpreted as follows: Instead of "filling the gaps" outside of $\mathcal{K}$, $\mathcal{K}$ is "dilated" by mapping it to the whole interval $[0, 1]$, using a famous singular function: The "Devil's staircase." One thus obtains the Lebesgue–Davenport function $\mathcal{L}_3$ which is considered in [13] (Example 5 of Chapter 10), and can be directly defined in a very simple way as follows: Let $t \in [0, 1)$ and

$$t = (0; t_1, t_2, \ldots, t_n, \ldots)_2 \tag{16}$$

be its proper expansion in the binary system. Then $\mathcal{L}_3(t) = (x_3(t), y_3(t))$, where

$$\begin{cases} x_3(t) = (0; t_1, t_3, t_5, \ldots)_2, \\ y_3(t) = (0; t_2, t_4, t_6, \ldots)_2. \end{cases} \tag{17}$$

One extends $\mathcal{L}_3$ to $t = 1$ by picking $\mathcal{L}_3(1) = (1, 1)$.

Let us first state precisely the relationship that we already mentioned between $\mathcal{L}_3$ and $\mathcal{L}_1$ or $\mathcal{L}_2$. Recall that the restriction of the Devil's staircase to $\mathcal{K}$ is defined as follows:

$$\text{If} \quad t = (0; 2t_1, 2t_2, \ldots, 2t_n, \ldots)_3, \quad \text{then} \quad \mathcal{D}(t) = (0; t_1, t_2, t_3, \ldots)_2.$$

Note that this restriction is onto $[0, 1]$ but is not one to one. It follows immediately from (12) and (17) that

$$\forall t \in \mathcal{K}^*, \quad \mathcal{L}_1(t) = \mathcal{L}_3 \circ \mathcal{D}(t).$$

As a consequence of this formula and of Lemma 10, it follows that $\mathcal{L}_3$ is onto $[0, 1]^2$.

The first step in order to study its properties is to rewrite it as a *Davenport series*. Let us start by recalling the definition of such series. They are odd 1-periodic functions of a particular type. Let $\{x\}$ be the "sawtooth function"

$$\{x\} = x - [x] - \frac{1}{2}.$$

Davenport series are of the form

$$\sum_{n=1}^{\infty} a_n \{nx\}; \tag{18}$$

in order to cover the case of space-filling functions, we will assume that $a_n \in \mathbb{R}^d$. We will only consider the case where $(a_n) \in l^1$, so that the series is normally convergent. Such series already occurred in the famous "Habilitationschrift" of Riemann, see [21,36], as an example of a Riemann-integrable function which is not Cauchy-integrable. Under their general form, they were first studied in 1936 by H. Davenport, see [11,12]; recent results on Davenport series can be found in [6,19].

Proposition 19. *The Lebesgue–Davenport function $\mathcal{L}_3$ has the following expansion*:

$$\begin{cases} x_3(t) = \frac{1}{2} + \sum_{n=0}^{\infty} a_n \{2^n t\}, & \text{where } a_{2l} = 2^{-l} \text{ and } a_{2l+1} = -2^{-l-1}, \\ y_3(t) = \frac{1}{2} + \sum_{n=1}^{\infty} a_n \{2^n t\}, & \text{where } a_{2l} = -2^{-l} \text{ and } a_{2l+1} = 2^{-l}. \end{cases} \tag{19}$$

Proof. Let $\omega(t)$ be the one periodic function such that

$$\begin{cases} \omega(t) = 0 & \text{if } t \in [0, \frac{1}{2}), \\ \omega(t) = 1 & \text{if } t \in [\frac{1}{2}, 1). \end{cases}$$

If t_n $(= t_n(t))$ is defined by (16), then

$$t_n(t) = \omega\big(2^{n-1} t\big);$$

thus

$$x_3(t) = \sum_{n=0}^{\infty} \frac{\omega(2^{2n} t)}{2^{n+1}} \quad \text{and} \quad y_3(t) = \sum_{n=0}^{\infty} \frac{\omega(2^{2n+1} t)}{2^{n+1}}.$$

Since

$$\omega(t) = 2\{t\} - \{2t\} + \frac{1}{2},$$

Proposition 19 follows immediately. □

Recall that *p-adic Davenport series* are series of the form

$$f(t) = \sum_{j=1}^{\infty} a_j \big\{p^j t\big\}, \tag{20}$$

where p is an integer larger than 2. Thus the coordinates of $\mathcal{L}_3$ are examples of dyadic Davenport series.

The following result is a particular case of Proposition 12 of [19], which yields the spectrum of singularities of p-adic Davenport series.

Proposition 20. *The spectrum of singularities of the Lebesgue–Davenport function $\mathcal{L}_3$ is given by*

$$d_3(H) = \begin{cases} 2H & \text{if } 0 \leqslant H \leqslant 1/2, \\ -\infty & \text{else.} \end{cases} \tag{21}$$

This result was not obtained through the everywhere determination of the Hölder exponent of such Davenport series, but as a consequence of general upper and lower bounds of their spectra; we will now sharpen this study by determining the exact pointwise regularity at every point of normally convergent p-adic Davenport series.

5.1. Pointwise regularity of p-adic Davenport series

We will assume in the following that $(a_j) \in l^1$; then the function f defined by (20) is the sum of a normally convergent series; it follows that it is continuous at every non p-adic real number, and has a right and a left limit at every p-adic rational kp^{-l} (where $k \wedge p = 1$), with a jump of amplitude

$$b_l = a_l + a_{l+1} + \cdots.$$

A sequence $(b_l)_{l\in\mathbb{N}}$ is called *regular* if

$$\exists C>0:\ \forall l \quad |b_l| \geqslant C \sup_{m\geqslant l} |b_m|. \tag{22}$$

Theorem 21. *Let f be given by* (20)*, with $a_j \in l^1$, and assume that its sequence of jumps is regular. Let $t_0 \in \mathbb{R}$; if t_0 is not a p-adic rational, let $\Delta_j(t_0) = \operatorname{dist}(t_0, p^{-j}\mathbb{Z})$, then*

$$h_f(t_0) = \liminf_{j\to\infty}\left(\frac{\log(|b_j|)}{\log(\Delta_j(t_0))}\right).$$

Assume now that $t_0 = kp^{-l}$ with $k\wedge p = 1$. If $b_l \neq 0$ then $h_f(t_0) = 0$, else

$$h_f(t_0) = \liminf_{j\to\infty}\left(\frac{\log(|b_j|)}{\log(p^{-j})}\right).$$

Theorem 21 yields the pointwise Hölder exponent of $\mathcal{L}_3$ at every point; indeed, the sequence of its triadic coefficients given by (19) obviously satisfies (22).

We will use the following lemma (Lemma 1 of [17]) which yields an upper bound for the Hölder exponent of any function having a dense set of discontinuities.

Lemma 22. *Let f be a locally bounded function; let $t_0 \in \mathbb{R}$ and let r_n be a sequence converging to t_0 such that, at each point r_n, f has a right and a left limit; then*

$$h_f(x_0) \leqslant \liminf\left(\frac{\log|f(r_n^+) - f(r_n^-)|}{\log|r_n - t_0|}\right).$$

We will also need the following lemma.

Lemma 23. *Let $\omega > 0$. There exists $C > 0$ such that*

$$\forall t_0,\ \forall L\in\mathbb{N},\quad \sum_{j=L}^{\infty}\big(\Delta_j(t_0)\big)^{\omega} \leqslant C\big(\Delta_L(t_0)\big)^{\omega}\big|\log\big(\Delta_L(t_0)\big)\big|.$$

Proof. Let M be such that:

$$p^{-M-1} < \Delta_L(t_0) \leqslant p^{-M}.$$

Then $M \geqslant L$ and, if $j \geqslant M$, since $\Delta_j(t_0) \leqslant p^{-j}$,

$$\sum_{j>M} \Delta_j(t_0)^{\omega} \leqslant \sum_{j>M} p^{-j\omega} \leqslant Cp^{-M\omega} \leqslant C\Delta_L(t_0)^{\omega}.$$

If $L \leqslant j \leqslant M$, since $\Delta_j(t_0)$ is decreasing,

$$\sum_{j=L}^{M} \Delta_j(t_0)^{\omega} \leqslant M\Delta_L(t_0)^{\omega} \leqslant C\big(\Delta_L(t_0)\big)^{\omega}\big|\log\big(\Delta_L(t_0)\big)\big|. \qquad \square$$

Proof of Theorem 21. We first consider the case where t_0 is not p-adic. The discontinuity of f at a point k/p^l, where $k\wedge p = 1$ has an amplitude b_l; we pick for r_n the sequence of dyadic points k/p^l that are closest to t_0. Either $k\wedge p = 1$ and the jump at that point has amplitude b_l, or $k\wedge p \neq 1$ and the jump has an amplitude b_m for an $m < l$, which, using (22), is larger than Cb_l. It follows from Lemma 22 that

$$h_f(t_0) \leqslant \liminf_{l\to\infty}\left(\frac{\log(|b_l|)}{\log(\Delta_l(t_0))}\right).$$

Let $h > 0$ be given and $I_h = [x_0 - h, x_0 + h]$. Let l be the integer defined by the conditions

$$\Delta_l(t_0) \leqslant h < \Delta_{l-1}(t_0). \tag{23}$$

The function $\{p^j t\}$ has no jump on I_h if $j < l$, so that

$$\sum_{j=0}^{l-1} a_j\big(\{p^j t_0\} - \{p^j(t_0+h)\}\big) = h\sum_{j=0}^{l-1} a_j p^j. \tag{24}$$

Let m denote the integer such that

$$p^{-m-1} < h \leqslant p^{-m}. \tag{25}$$

It follows from the definition of Δ_l that $m > l$. If $l \leqslant j < m$, then $\{p^j t\}$ has exactly one jump on I_h, so that

$$\sum_{j=l}^{m-1} a_j\big(\{p^j t_0\} - \{p^j(t_0+h)\}\big) = h\sum_{j=l}^{m-1} a_j p^j - \sum_{j=l}^{m-1} a_j = h\sum_{j=l}^{m-1} a_j p^j - b_l + \sum_{j=m}^{\infty} a_j. \tag{26}$$

Finally, since $\{p^j t\} \leqslant 1/2$, it follows that

$$\left|\sum_{j=m}^{\infty} a_j\big(\{p^j t_0\} - \{p^j(t_0+h)\}\big)\right| \leqslant \sum_{j=m}^{\infty} |a_j|. \tag{27}$$

It follows from (24), (26) and (27) that

$$f(t_0) - f(t_0+h) = \sum_{j=0}^{\infty} a_j\big(\{p^j t_0\} - \{p^j(t_0+h)\}\big) = h\sum_{j=0}^{m-1} a_j p^j - b_l + \mathcal{O}\left(\sum_{j=m}^{\infty} |a_j|\right). \tag{28}$$

Let $A = \liminf_{j\to\infty} \frac{\log(|b_j|)}{\log(\Delta_j(t_0))}$ and let $\omega < A$, which can be arbitrarily close to A. In order to prove Theorem 21, we will bound each term of (28) by $h^\omega|\log(\omega)|$. By definition of A, for j large enough, $|b_j| \leqslant \Delta_j(t_0)^\omega$. In particular,

$$|b_l| \leqslant \Delta_l(t_0)^\omega \leqslant h^\omega.$$

Since $a_j = b_j - b_{j+1}$, it follows that $|a_j| \leqslant 2\Delta_j(t_0)^\omega$, and it follows from Lemma 23 that

$$\sum_{j=m}^{\infty} |a_j| \leqslant 2\sum_{j=m}^{\infty} |b_j| \leqslant \sum_{j=m}^{\infty} \Delta_m(t_0)^\omega \leqslant C\big(\Delta_m(t_0)\big)^\omega \big|\log\big(\Delta_m(t_0)\big)\big| \leqslant Cmp^{-m\omega},$$

which, by (25) is bounded by $h^\omega|\log(\omega)|$.

Let us now estimate the first term in the right-hand side of (28).

- If $A \leqslant 1$, then we can pick $\omega < 1$, and

$$\sum_{j=0}^{m-1} |a_j| p^j \leqslant 2\sum_{j=0}^{m-1} |b_j| p^j \leqslant 2\sum_{j=0}^{m-1} \big(\Delta_j(t_0)\big)^\omega p^j \leqslant 2\sum_{j=0}^{m-1} p^{(1-\omega)j} \leqslant Cp^{(1-\omega)m} \leqslant Ch^{\omega-1}.$$

- If $A > 1$, then we can pick $\omega > 1$. We first notice that the series $\sum a_j p^j$ is absolutely convergent since the same estimate as above yields that its general term is bounded by $p^{(1-\omega)j}$. Therefore, we can write

$$h\sum_{j=0}^{m-1} a_j p^j = h\left(\sum_{j=0}^{\infty} a_j p^j\right) - h\sum_{j=m}^{\infty} a_j p^j.$$

  The first term is a linear function of h, and the second one is bounded as above by

$$h\sum_{j=m}^{\infty} p^{(1-\omega)j} \leqslant Chp^{(1-\omega)m} \leqslant Ch^\omega.$$

We still have to consider the case of p-adic points. let $t_0 = \frac{k}{p^l}$ with $k \wedge p = 1$. If $b_l \neq 0$, then f has a jump at t_0 and the Hölder exponent of f vanishes at t_0. The case of a rational p-adic point where the jump vanishes is similar to the general case above, so that we omit its proof. □

6. Multifractal analysis based on ultrametric topologies

We will now show that, using an ultrametric distance on $[0,1]$, $\mathcal{L}_3$, and more generally p-adic Davenport series become monohölder functions. We get back to the setting supplied by (2), and we will use for distance the p-adic distance on $[0,1]$, which is the most natural in the setting of p-adic Davenport series.

Definition 24. Let $s, t \in [0,1)$, with the proper expansions in base p

$$s = (0; s_1, s_2, \ldots, s_n, \ldots)_p, \qquad t = (0; t_1, t_2, \ldots, t_n, \ldots)_p$$

respectively and $\delta_p(s,t) = \inf\{k\colon\ s_k \neq t_k\} - 1$. The p-adic distance between s and t is $d_p(s,t) = p^{-\delta_p(s,t)}$.

We first remark that the p-adic distance is an *increasing right-continuous ultrametric distance*, i.e. is an ultrametric distance satisfying the additional requirements

$$\begin{cases} \text{if } x \leqslant y \leqslant z \quad \text{then } d(x,z) = \max(d(x,y), d(y,z)), \\ \forall x, \quad \lim_{h \to 0^+} d(x, x+h) = 0. \end{cases}$$

These two requirements can be interpreted as follows: Among ultrametric distances, these one are "as close as possible" to the usual distance on $\mathbb{R}$. In the following of this section, functions are considered as mappings $f : (\mathbb{R}, d_p) \to (\mathbb{R}, d)$, where d_p is the p-adic ultrametric distance, whereas d is the usual distance. Recall that the finite differences of arbitrary order are defined as follows.

$$\big(\Delta_h^1 f\big)(x) = f(x+h) - f(x), \qquad \big(\Delta_h^{n+1} f\big)(x) = \big(\Delta_h^n f\big)(x+h) - \big(\Delta_h^n f\big)(x).$$

Regularity criteria in this setting are defined as follows.

Definition 25. Let $\alpha > 0$. A function $f : [0,1] \to \mathbb{R}$ belongs to $C_p^\alpha(x_0)$ if there exist $C > 0$ and a polynomial P of degree less than α such that

$$\forall x \in [0,1], \quad \big|f(x) - P(x - x_0)\big| \leqslant C\big(d_p(x, x_0)\big)^\alpha. \tag{29}$$

The p-adic Hölder exponent of f at x_0 is $h_f^p(x_0) = \sup\{\alpha\colon\ f \in C_p^\alpha(x_0)\}$.

A function f belongs to $C_p^\alpha([0,1])$ if there exists $C > 0$ such that, $\forall x_0 \in [0,1]$, (29) holds.

In the p-adic setting, one can also define a notion of uniform irregularity, which is similar to the one defined in Definition 5, except that in (8), the condition $y \in B(x,r)$ is replaced by $y \in B_p(x,r)$, where $B_p(x,r)$ denotes the p-adic ball of center x and radius r.

Definition 26. Let $\alpha > 0$. A function $f : [0,1] \to \mathbb{R}$ belongs to $I_p^\alpha([0,1])$ if there exists $C > 0$ such that, for any ball $B = B_p(x,r)$, and for $n = [\alpha] + 1$,

$$\sup_{y,\, y+nh \in B} \big|\big(\Delta_h^n f\big)(y)\big| \geqslant C r^\alpha. \tag{30}$$

Proposition 27. *Let f be given by* (20)*, with $a_j \in l^1$ and let $\alpha \in (0,1)$.*

- *If there exists $C > 0$ such that $|a_l| \leqslant C p^{-\alpha l}$, then $f \in C_p^\alpha([0,1])$.*
- *If there exists $C > 0$ such that for l large enough $|b_l| \geqslant C p^{-\alpha l}$, then $f \in I_p^\alpha([0,1])$.*

Proposition 19 implies that $\mathcal{L}_3$, considered as a function defined on $[0,1]$ endowed with the p-adic distance, is a monohölder function of exponent $1/2$. In order to prove Proposition 27, we will need the following lemma.

Lemma 28. *The mapping $x \to \{p^n x\}$ is Lipschitz, with Lipschitz constant bounded by $2p^n$.*

Proof. Let $x, y \in [0,1]$ and let l be such that $d_p(x,y) = p^{-l}$; then x and y are in the same p-adic interval of length p^{-l} so that $|x - y| \leqslant p^{-l}$; therefore

$$\forall x, y\colon \quad |x - y| \leqslant d_p(x,y). \tag{31}$$

If $l \leqslant n$, then

$$\big|\{p^n x\} - \{p^n y\}\big| \leqslant 2 \leqslant 2p^n d_p(x,y).$$

If $l > n$, then $2^n x$ and $2^n y$ are in the same p-adic interval of length p^{n-l} and $\{p^n x\}$ is linear on this interval, so that

$$\big|\{p^n x\} - \{p^n y\}\big| \leqslant p^n |x - y| \leqslant 2p^n d_p(x,y). \qquad \square$$

Proof of Proposition 27. The function f is the sum of a normally convergent series of continuous functions (for the p-adic distance) and is therefore continuous. If $|a_l| \leqslant \frac{C}{p^{\alpha l}}$ and if $d_p(x,y) = p^{-l}$, then

$$\big|f(x) - f(y)\big| \leqslant \sum_{n=0}^{l} |a_n| p^n d_p(x,y) + 2\sum_{l+1}^{\infty} |a_n| \leqslant C \sum_{n=0}^{l} p^{-\alpha n} p^n d_p(x,y) + C \sum_{n=l+1}^{\infty} p^{-\alpha n} \leqslant C p^{-\alpha l} \leqslant C d_p(x,y)^\alpha.$$

We now prove the second part of the proposition. Consider an open p-adic interval $I_{k,l-1}$ of length p^{-l+1}. At each p-adic rational kp^{-l} inside this interval, the jump of f is b_l, and therefore there exist points x, y arbitrary close to kp^{-l} and which lie on each side of it and such that $|f(x) - f(y)| \geqslant |b_l|/2$. The second part of the proposition follows. $\square$

7. Numerical results concerning the multifractal formalisms

The numerical determination of the spectrum of singularities of a signal is derived through the application of a multifractal formalism; in such formulas, the spectrum is obtained through a Legendre transform of a "scaling" function which is computable on real life data. The variants depend on the use of different scaling functions, so that the accuracy of the method depends on two conditions: A theoretical one, the validity of the multifractal formalism used, and a practical one, the properties of the scaling function used, and the way it is discretized. Its estimation relies on parameters (e.g. the number of points used to sample the signal, the error in the measurements) that are often hard to handle. A natural way to determine whether or not a method is an effective one is to test it on a collection of mathematical functions or stochastic processes whose multifractal spectra are theoretically known. In the following, we recall the two most reliable numerical methods which have been implemented in order to estimate the entire spectrum and we test their accuracy on the functions introduced above.

7.1. Definition of the WTMM and the WLM

The two formalisms we will review here are inspired by the one of Parisi and Frisch [32]; its principium is to estimate the spectrum of singularities from global quantities, easily computable: the L^q-norms of the increments. The main drawback of this method is that it is meaningless for negative values of q and, as a consequence, can only lead, at best, to the increasing part of the spectrum. Some attempts were made to fix this problem, but none really succeeded (see [5,27]).

To overcome the difficulties raised by the negative values of q, Arneodo et al. proposed a wavelet-based method: the *wavelet transform maxima method* (WTMM), see [3]. The idea is to replace the increments with a wavelet and to get rid of null or small values by only retaining the maxima of the continuous wavelet transform. We will suppose that the function $\psi \in L^1 \cap L^\infty(\mathbb{R})$ is either even or odd. Such a "wavelet" is r-smooth if $\psi \in C^r(\mathbb{R})$, if its r first moments vanish, and if the $\partial^s \psi$ have fast decay ($s \leqslant r$). The continuous wavelet transform of a function $f \in L^2(\mathbb{R})$ is defined as follows,

$$W_f(b,a) = \frac{1}{a}\int f(x)\psi\left(\frac{x-b}{a}\right)dx.$$

The WTMM is computed using the notion of line of maxima. For some $a \in [a', a'']$, we write $l_a = |W(b_0, a)|$ if b_0 is a local maximum of the function $b \mapsto |W(b,a)|$. These local maxima are tracked and linked through the scales to yield lines of maxima l_a which are replaced by the quantity

$$m_a = \sup_{a' \leqslant a} l_{a'}.$$

The *partition function* associated with the lines of maxima is

$$S_\tau(a,q) = \sum_l m_a^q,$$

where the sum is taken over all the lines of maxima reaching the scale a. We then set

$$\tau(q) = \liminf_{a\to 0} \frac{\log S_\tau(a,q)}{\log a} \tag{32}$$

to obtain the spectrum of singularities from the following relation:

$$d_\tau(h) = \inf_q \{hq - \tau(q)\}.$$

Using the maxima for the computation of S_τ prevents the presence of null values in the wavelet transform.

More recently, a similar approach based on the discrete wavelet transform was introduced: the *wavelet leaders method* (WLM), see [18]. Let us recall some definitions (see [1,18]). From now on, we will denote by λ the dyadic interval $\lambda = \lambda(j,k) = \left[\frac{k}{2^j}, \frac{k+1}{2^j}\right]$. One uses r-smooth wavelets ψ such that $\{2^{j/2}\psi(2^j x - k)\colon\ j,k \in \mathbb{Z}\}$ is an orthonormal basis of $L^2(\mathbb{R})$. Therefore, any function $f \in L^2(\mathbb{R})$ can be written

$$f(x) = \sum_{j,k\in\mathbb{Z}} c_\lambda \psi\left(2^j x - k\right),$$

where $c_\lambda = 2^j \int f(x)\psi(2^j x - k)\,dx$. The wavelet leader associated to the dyadic interval λ is the quantity

$$d_\lambda = \sup_{\lambda' \subset 3\lambda} |c_{\lambda'}|.$$

We then define the partition function associated to the WLM

$$S_\omega(j,q) = 2^{-j} \sum_{\lambda\in\Lambda_j}{}^{*} d_\lambda^q, \tag{33}$$

where $\sum^*$ means that the sum is restricted to the intervals λ such that $\inf_{\lambda' \subset \Lambda(\lambda)} |c_{\lambda'}| \neq 0$, where $\Lambda(\lambda) = \{\lambda' :\ \lambda' \subset \lambda\} \cup \{\lambda' :\ \lambda \subset \lambda'\}$. This restriction is made in order to avoid, as much as possible, the presence of small, numerically instable, coefficients. The sum is taken over all intervals λ belonging to $\Lambda_j = \{\lambda :\ \operatorname{diam}(\lambda) = 2^{-j}\}$. From this, we set

$$\omega(q) = \liminf_{j \to \infty} \frac{\log S_\omega(j, q)}{\log 2^{-j}} \tag{34}$$

to obtain the spectrum of singularities as

$$d_\omega(h) = \inf_q \big\{ hq - \omega(q) \big\}. \tag{35}$$

The heuristic argument from which the preceding methods are derived is the following (we describe it for the WLM, but it can be transposed to the WTMM). Equality (34) means $\sum^* d_\lambda^q \sim 2^{-\omega(q) j}$. The contribution of the dyadic intervals $\lambda \in \Lambda_j$ containing a point whose Hölder exponent is h to the sum $\sum^* d_\lambda^q$ can be estimated as follow. If $\lambda_j(x) \in \Lambda_j$ is the interval at scale j containing x, the Hölder exponent $h(x)$ of f at x is given by

$$h(x) = \liminf_{\substack{j \to \infty \\ \lambda' \subset 3\lambda_j(x)}} \frac{\log d_{\lambda'}}{\log 2^{-j}} \tag{36}$$

(see [18]). Therefore, one has $d_\lambda \sim 2^{-hj}$. Moreover, the number of these dyadic intervals λ should be about $2^{d_\omega(h) j}$, where d_ω is the multifractal spectrum of the function. Hence, the contribution is

$$2^{(d_\omega(h) - hq) j}. \tag{37}$$

The dominating contribution is the one corresponding to a value of h associated with the biggest exponent in (37); thus, one can expect the following relation

$$-\omega(q) = \sup_h \big\{ d_\omega(h) - hq \big\}.$$

As $-\omega$ is a convex function, if d_ω is concave, then $-\omega$ and $-d_\omega$ are convex conjugate functions, so that (35) holds. Let us remark that the preceding argument is far from being a mathematical proof. The only result valid in the general case is the following inequality, see [18],

$$d_\omega(h) \leqslant \inf_q \big(hq - \omega(q) \big). \tag{38}$$

These two formalisms are the only ones that can lead to the entire spectrum of singularities (i.e. that allow to obtain the decreasing part of the spectrum). The main advantage of the WLM is its theoretical background. In particular, relation (36), used in the derivation of the multifractal formalism, does not hold in general for wavelet maxima. The WLM could also be more efficient in the characterization of the regularity of signals with oscillating singularities, a domain where the WTMM never succeeded. Moreover the WLM is faster than the WTMM, since the complexity of the WLM is linear, while the order of complexity of the WTMM is at least $N \log N$ (indeed, the computational speed of the two-dimensional WTMM can be a real problem). However, the WTMM has been successfully applied to numerous applications, going from DNA sequences to stock market data analysis (see e.g. [2]). It is translation invariant, a property that the WLM does not have. Moreover, the use of a starred sum in (33) can induce an important loss of coefficients in the definition of S_ω. This can lead to unsatisfactory results when applied to functions such as the devil staircase.

7.2. Multifractal formalisms applied to $\mathcal{L}_1$, $\mathcal{L}_2$ and $\mathcal{L}_3$

We show here that the WLM applied to highly irregular functions gives at least the same positive results, but in a much faster way. However, some problems can arise if too many wavelet leaders vanish.

To test and compare the efficiency of the two methods, we have computed the functions $\mathcal{L}_1$, $\mathcal{L}_2$ and $\mathcal{L}_3$ with sample sizes ranging from $S = 2^{14}$ to $S = 2^{22}$. We have limited the study of the functions τ and ω within the range $-3 \leqslant q \leqslant 5$ (as we will see, there is no need to extend the study for larger range when considering these specific Lebesgue-type functions). For both methods, wavelets with exactly two vanishing moments were used: the second-order derivative of the Gaussian function for the WTMM and the second-order Daubechies wavelet for the WLM (let us recall that the Daubechies wavelets are compactly supported, see [10]). The results remain unchanged if wavelets with a higher number of vanishing moments are chosen. For a fixed q, $\tau(q)$ and $\omega(q)$ are obtained through a linear regression, following (32) and (34), respectively.

The function $\mathcal{L}_2$ is a monohölder function. The associated multifractal spectrum is thus the simplest spectrum we have obtained, since it is reduced to a single point:

$$d_2(h) = \begin{cases} 1 & \text{if } h = \frac{\log 2}{2 \log 3} = 0.31546\ldots, \\ -\infty & \text{else.} \end{cases}$$

As shown in Fig. 6 for sample size $S = 2^{14}$, both the functions τ and ω display a remarkable linear behavior, which is the mark of a monohölder function. The Hölder exponent h is then obtained through a linear regression. The WTMM gives

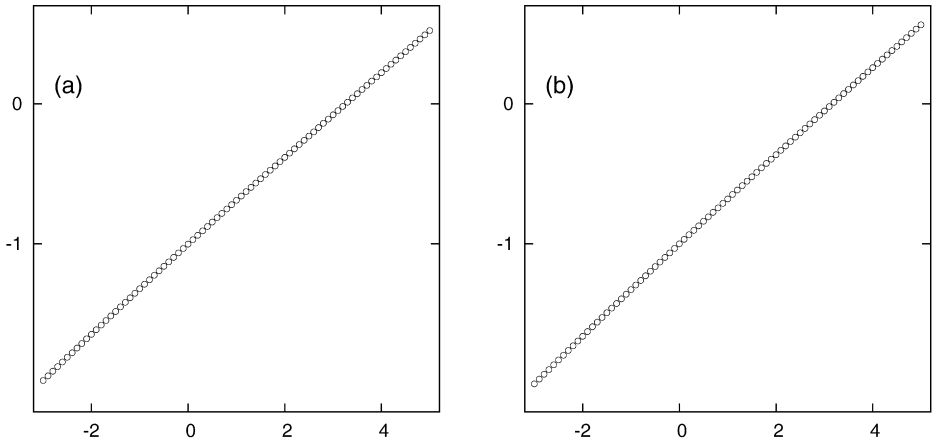

Fig. 6. (a) The estimated function τ associated to the Schoenberg function $\mathcal{L}_2$. (b) The estimated function ω.

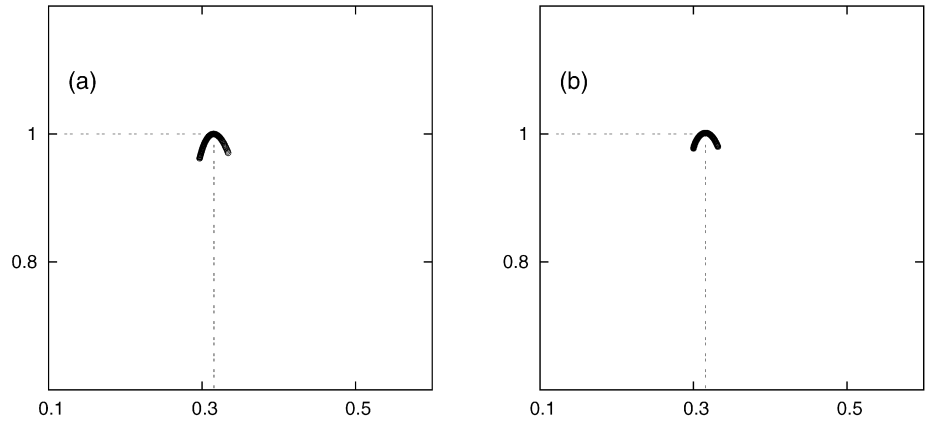

Fig. 7. (a) The spectrum of singularities of $\mathcal{L}_2$ estimated through the function τ (see Fig. 6). (b) The spectrum obtained using ω. The dashed lines intersect at $(\frac{\log 2}{2\log 3}, 1)$.

$h_\tau \approx 0.311 \pm 0.024$ and the WLM gives $h_\omega \approx 0.319 \pm 0.024$. In both case, the error is close to 4.1×10^{-3}. Fig. 7 shows the spectra of singularities obtained from τ and ω respectively, through a Legendre transform.

The function $\mathcal{L}_1$ is monofractal but not monohölder:

$$d_1(h) = \begin{cases} \frac{\log 2}{\log 3} & \text{if } h = \frac{\log 2}{2\log 3}, \\ 1 & \text{if } h = \infty, \\ -\infty & \text{else.} \end{cases}$$

However, if a compactly supported wavelet with more than one vanishing moment is used to perform the wavelet transform, the coefficients corresponding to the C^∞ component, i.e. the linear parts of $\mathcal{L}_1$, are equal to zero. Since the lines of maxima are made of maxima of the modulus of the continuous wavelet transform, such coefficients are not taken into account in the WTMM. For the WLM, vanishing coefficients have to be dropped to compute the partition function. This operation must be done carefully. The best method seems to be using the starred sum in the formula (33), after having set to zero the coefficients beyond a fixed threshold, which should correspond to a numerical accuracy. In the case of $\mathcal{L}_1$, this threshold is naturally obtained by checking the values of the coefficients at the lowest scale corresponding to the interval $]\frac{1}{3}, \frac{2}{3}[$. Since, these coefficients should vanish, the threshold must be larger than their numerical value, which is a computational artifact. The main disadvantage of this "starred sum method" is that, in some special situations, many coefficients can be lost, as it is the case with $\mathcal{L}_1$. Although this algorithm is satisfactory when applied to the functions studied here, it could be interesting to define the threshold as a function of the scale.

Since vanishing coefficients are not taken into account, both the WTMM and the WLM are only performed on the function $\mathcal{L}_1$ restricted to the Cantor set $\mathcal{K}$, which is a monohölder function. The so-obtained spectrum of singularities is thus reduced to one single point. If the wavelet has only one vanishing moment, one can show that the multifractal formalism will lead to a wrong spectrum (see [28]). Both τ and ω display the expected linear behavior when working with the sample size $S = 2^{20}$, as shown in Fig. 8. One gets $h_\tau \approx 0.339 \pm 0.03$ and $h_\omega \approx 0.335 \pm 0.02$. When working with a smaller

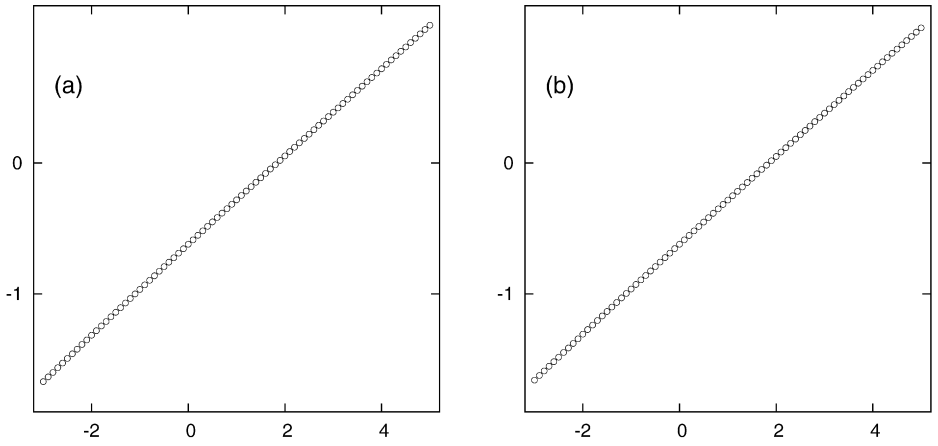

Fig. 8. (a) The estimated function τ associated to the Lebesgue function $\mathcal{L}_1$. (b) The estimated function ω.

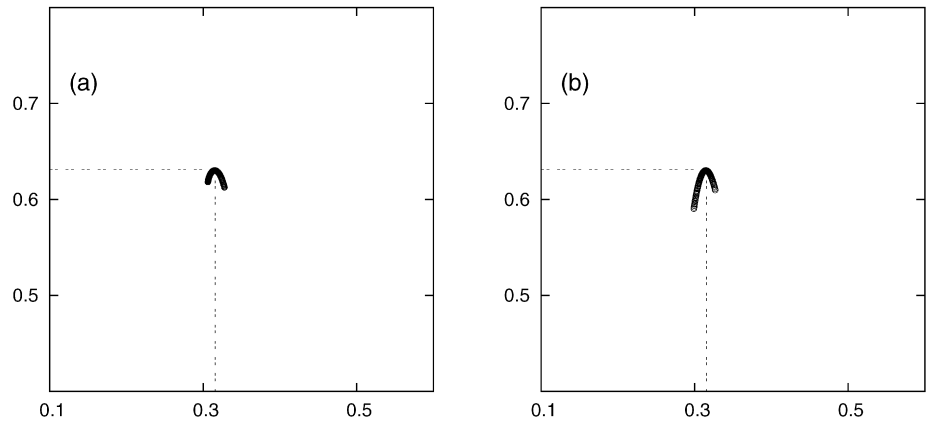

Fig. 9. (a) The spectrum of singularities of $\mathcal{L}_1$ estimated through the function τ (see Fig. 8). (b) The spectrum obtained using ω. The dashed lines intersect at $\left(\frac{\log 2}{2\log 3}, \frac{\log 2}{\log 3}\right)$.

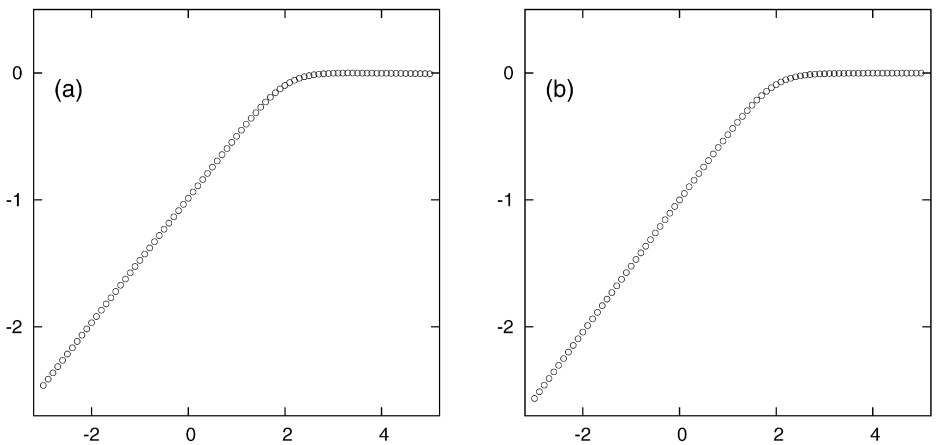

Fig. 10. (a) The estimated function τ associated to the Lebesgue–Davenport function $\mathcal{L}_3$. (b) The estimated function ω.

sample size ($S = 2^{14}$), the corresponding τ still display a linear behavior with an overestimated exponent ($h_\tau \approx 0.4 \pm 0.015$), while no such linear behavior is observed for ω.

The Lebesgue–Davenport function $\mathcal{L}_3$ is neither monohölder nor monofractal; the associated spectrum of singularities is given by Proposition 20. Both τ and ω display a satisfactory shape when working with the smallest sample size $S = 2^{14}$, but a sample size of $S = 2^{20}$ is needed to estimate the maximum Hölder exponent with a precision of 2% (the maximum

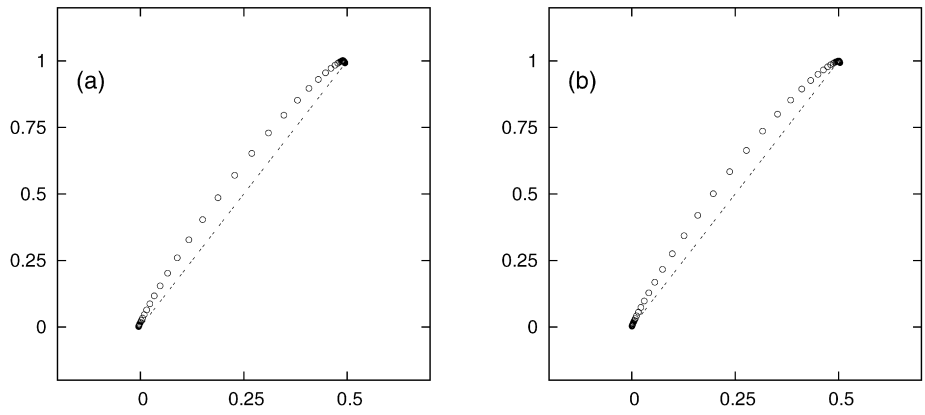

Fig. 11. (a) The spectrum of singularities of $\mathcal{L}_3$ estimated through the function τ (see Fig. 10). (b) The spectrum obtained using ω. The real spectrum d_3 is plotted with dashed lines.

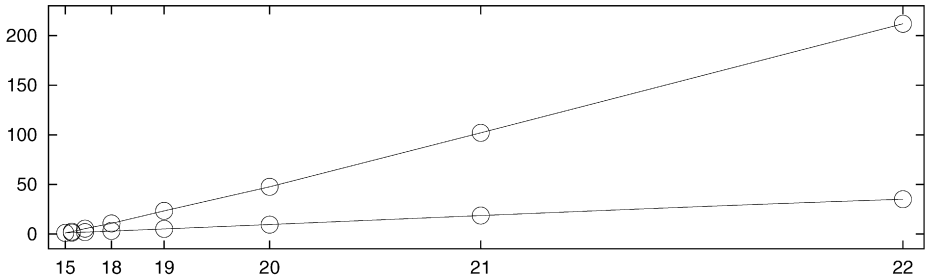

Fig. 12. The relative computational speeds of the WTMM and the WLM tested on the function $\mathcal{L}_3$ with sample sizes $S = 2^{15}, 2^{16}, \ldots, 2^{22}$.

Hölder exponent is simply obtained from τ or ω through a linear regression over the negative values of q, see Fig. 10). As shown in Fig. 11, both formalisms lead to a strictly concave spectrum whose shape is close to the exact linear spectrum. Recall that d_3 has a dense set of discontinuities, so that the upper bound (38) is no more valid. In short, there is no theoretical background for multifractal functions. Under such condition, it is quite remarkable that the numerical results obtained are not too far from the theoretical spectrum.

In conclusion, we can say that the WTMM and the WLM give the same, correct, results on the tested functions, but some problems can arise with the WLM when the discrete wavelet transform contains too many vanishing coefficients. The main pitfall of the WTMM, beside the lack of theoretical foundation, is its computational speed and the quantity of memory needed. As shown in Fig. 12, when applied to the function $\mathcal{L}_3$ with a sample size equal to $S = 2^{22}$, the WTMM is about six times slower than the WLM.

References

[1] P. Abry, S. Jaffard, B. Lashermes, Wavelet leaders in multifractal analysis, in: T. Qian, et al. (Eds.), Wavelet Analysis and Applications, Birkhäuser, 2006, pp. 219–264.
[2] A. Arneodo, B. Audit, N. Decoster, J.-F. Muzy, C. Vaillant, Wavelet-based multifractal formalism: Applications to DNA sequences, satellite images of the cloud structure and stock market data, in: A. Bunde, J. Kropp, H.J. Schellnhuber (Eds.), The Science of Disasters, Springer, 2002, pp. 27–102.
[3] A. Arneodo, E. Bacry, J.-F. Muzy, The thermodynamics of fractals revisited with wavelets, Physica A 213 (1995) 232–275.
[4] J. Alsina, The Peano curve of Schoenberg is nowhere differentiable, J. Approx. Theory 33 (1981) 28–42.
[5] A.L. Barabási, T. Vicsek, Multifractality of self-affine fractals, Phys. Rev. E 44 (1991) 2730–2733.
[6] A.S. Belov, On the Salem and Zygmund problem with respect to the smoothness of an analytic function that generates a Peano curve, Math. USSR-Sb. 70 (2) (1991) 485–497.
[7] S. Biswas, Hilbert scan and image compression, in: IEEE Int. Conf. Pattern Recogn., 2000, pp. 201–220.
[8] T. Bousch, Y. Heurteaux, Caloric measure on domains bounded by Weierstrass-type graphs, Ann. Acad. Sci. Fenn. 25 (2) (2000) 501–522.
[9] M. Clausel, Notions d'irrégularité uniforme et ponctuelle, preprint, 2007.
[10] I. Daubechies, Ten Lectures on Wavelets, SIAM, 1992.
[11] H. Davenport, On some infinite series involving arithmetical functions, Quart. J. Math. 8 (1937) 8–13.
[12] H. Davenport, On some infinite series involving arithmetical functions II, Quart. J. Math. 8 (1937) 313–320.
[13] B.R. Gelbaum, J.M.H. Olmsted, Counterexamples in Analysis, Holden Day Inc., San Francisco, 1965.
[14] D. Hilbert, Über die stetige Abbildung einer linie auf ein Flächenstück, Math. Ann. 38 (1891) 459–460.
[15] J.-B. Hiriart-Urruti, Une courbe étrange venue d'ailleurs, Rev. Math. Spé. (1986) 229–230.
[16] S. Jaffard, Multifractal Formalism for Functions, Parts I and II, vol. 28, SIAM, 1997, pp. 945–998.
[17] S. Jaffard, Old friends revisited. The multifractal nature of some classical functions, J. Fourier Anal. Appl. 3 (1997) 1–22.
[18] S. Jaffard, Wavelet techniques in multifractal analysis, in: M. Lapidus, M. van Frankenhuijsen (Eds.), Fractal Geometry and Applications: A Jubilee of Benoit Mandelbrot, Proceedings of Symposia in Pure Mathematics, vol. 72, AMS, 2004, Part 2, pp. 91–152.

[19] S. Jaffard, On Davenport expansions, Proc. Sympos. Pure Math. 72 (1) (2004) 273–303.
[20] S. Jaffard, B. Mandelbrot, Local regularity of nonsmooh wavelet expansions and application to the Polya function, Adv. Math. 120 (1996) 265–282.
[21] J.-P. Kahane, P.-G. Lemarié, Séries de Fourier et Ondelettes, Cassini, 1998.
[22] B. Lashermes, D. Roux, P. Abry, S. Jaffard, Comprehensive multifractal analysis of turbulent velocity using the wavelet leaders, Eur. Phys. J., in press.
[23] J. Lawder, The application of space-filling curves to the storage and retrieval of multidimensional data, PhD thesis, School of Comp. Sci. and Inf. Syst. Univ. of London, 2000.
[24] H. Lebesgue, Leçons sur l'integration et la recherche de fonctions primitives, Gautiers–Villars, 1904.
[25] B. Mandelbrot, Fractals and Scaling in Finance, Springer, 1997.
[26] B. Mandelbrot, S. Jaffard, Peano–Pólya motions, when time is intrinsic or binomial (uniform or multifractal), Math. Intelligencer 19 (1997) 21–26.
[27] J.F. Muzy, E. Bacry, A. Arneodo, Multifractal formalism for signals: The structure-function approach versus the wavelet-transform modulus-maxima method, Phys. Rev. E 47 (1993) 875–884.
[28] J.F. Muzy, Analyse de distributions fractales à partir de leur transformée en ondelettes, Ann. Phys. Fr. 20 (1995) 63–231.
[29] E.H. Moore, On certain crinkly curves, Trans. Amer. Math. Soc. 1 (1900) 72–90.
[30] M. Morayne, On differentiability of Peano-type functions (I and II), Colloq. Math. 53 (1987) 129–135.
[31] S. Nicolay, Analyse de séquences ADN par la transformée en ondelettes : Extraction d'informations structurelles, dynamiques et fonctionnelles, Thèse de l'Université de Liège, 2006.
[32] G. Parisi, U. Frisch, On the singularity spectrum of fully developed turbulence, in: Turbulence and Predictability in Geophysical Fluid Dynamics, Proceedings of the International Summer School in Physics Enrico Fermi, North-Holland, 1985, pp. 84–87.
[33] S. Patil, S. Das, A. Nasipuri, Serial data fusion using space-filling curves in wireless sensor networks, in: Proc. IEEE Conf. SECON, Santa Clara, CA, 2005.
[34] G. Peano, Sur une courbe, qui remplit toute une aire plane, Math. Ann. 36 (1890) 157–160.
[35] J. Quinqueton, M. Berthod, A locally adaptive Peano scanning algorithm, IEEE Trans. Pattern Anal. Mach. Intell. 3 (1981) 409–412.
[36] B. Riemann, Über die Darstellbarkeit einer Funktion durch eine trigonometrische Reihe, Habilitation thesis (1854), in: Collected Works of Bernard Riemann, Dover Pub. Inc., 1953.
[37] H. Sagan, Space Filling Curves, Springer, 1994.
[38] R. Salem, A. Zygmund, Lacunary power series and Peano curves, Duke J. 12 (1945) 569–578.
[39] I.J. Schoenberg, The Peano curve of Lebesgue, Bull. Amer. Math. Soc. 44 (1938) 519.
[40] S. Seuret, On multifractality and time subordination for continuous functions, preprint, 2007.
[41] W. Sierpiński, Sur une nouvelle courbe continue qui remplit toute une aire plane, Bull. Ann. Sci. Cracov. (1912) 462–478.
[42] H. Steinhaus, La courbe de Peano et les fonctions indépendantes, C. R. Acad. Sci. Paris 202 (1936) 1961–1963.
[43] W. Wunderlich, Über Peano-Kurven, Elem. Math. 28 (1973) 1–10.